Polarization conversions of diffractive wave plates based on orthogonal circular-polarization holography

Peng Cai (蔡 鹏)[1], Jianhao Wang (王健豪)[2], Changshun Wang (王长顺)[1,*], Pengfei Zeng (曾鹏飞)[1], and Hongjing Li (李洪婧)[1]

[1]*State Key Laboratory of Advanced Optical Communication Systems and Networks, Department of Physics and Astronomy, Shanghai Jiao Tong University, Shanghai 200240, China*
[2]*Shanghai Key Laboratory of Green Chemistry and Chemical Processes, Department of Chemistry, East China Normal University, Shanghai 200062, China*
**Corresponding author: cswang@sjtu.edu.cn*

Received July 21, 2015; accepted November 26, 2015; posted online January 6, 2016

A polarization holographic grating, which integrates the functions of a grating and a wave plate and is called a diffractive wave plate, is recorded by two beams (left and right circularly polarized) of a 532 nm laser in an azo polymer with a liquid-crystal structure. The polarization conversion characteristics of the diffractive wave plates are investigated with a detecting light of 650 nm by metering the polarization state of first-order diffracted light. It is confirmed that the diffractive wave plates convert the incident linear polarization into circular polarization for a linearly polarized probe laser and reverse the sense of rotation of the circular polarization when the detecting light is circularly polarized light.

OCIS codes: 090.0090, 090.2880, 260.5430.
doi: 10.3788/COL201614.010009.

As we know, wave plates and diffraction gratings are two different kinds of optical components. A wave plate alters the polarization state of an incident laser beam. A diffraction grating splits the incident light into several beams, and diffracts them to different directions. So a traditional optical device cannot realize these two functions at the same time. But if the grating is also a wave plate, the functions of the two optical components can be combined. Such optical components are called "diffractive wave plates,"[1] and they are essentially polarization holography gratings, which will be very useful for the preparation of multifunctional diffractive optical elements and all-optical devices[2,3].

Polarization holographic gratings can be recorded in polarization-sensitive mediums by two beams of orthogonal circularly polarized light. The resulting light fields of this type are modulated by polarization only, and a spatially modulated anisotropy is induced in the recorded medium[4,5]. There are various types of polarization-sensitive materials suitable for recording polarization holographic gratings, such as spirooxazine doped polymers, Ag/TiO_2 nanocomposite films, and azo materials[6–9]. Among these, the polymer containing a side chain of azobenzene has been extensively studied for its superior photosensitive properties during recording and long-term stability after recording[10–16]. Ono *et al.* have discussed the polarization state transformation of polarization gratings both experimentally and theoretically[17]. They used half-wave plates and quarter-wave plates to measure the polarization state of the recorded gratings point by point, which is tedious and cannot be done in real time. In this Letter, we use a polarimeter connected to a computer to detect the polarization state of the beam in real time and meter, and summarize the polarization conversion properties of a diffractive wave plate fabricated by two orthogonally circularly polarized continuous lasers using polarization holographic techniques.

Our sample is composed of an azo-free Polymer (A) and an azo-containing Polymer (B). Figures 1 and 2 show the molecular structure and absorption spectrum, respectively. Because of its low glass transition temperature (48.7°C), the sample can be prepared as follows: by putting some sample powder between two pieces of glass slides, heating it to 100°C, and then allowing it to cool to room temperature naturally, while applying suitable pressure at the same time, a sample is successfully prepared[18]. The thickness of the sample film is about 15 μm.

Figure 3 shows the experimental setup for studying the photo-induced birefringence effect. A continuous 532 nm laser is used to induce the birefringence; due to the 532 nm wavelength, it is absorbed well by the sample. A continuous 650 nm laser is used to probe the birefringence in real time because the 650 nm laser is not absorbed by the sample. The polarization angles of P_1 and P_2 are set to be

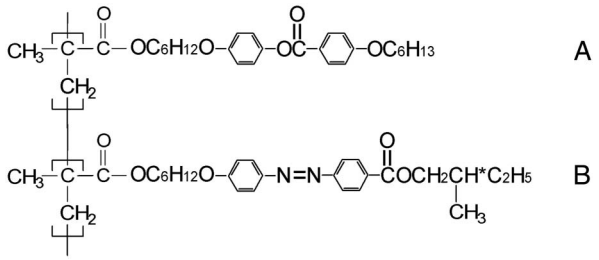

Fig. 1. Molecular structure of the azobenzene liquid-crystalline polymer.

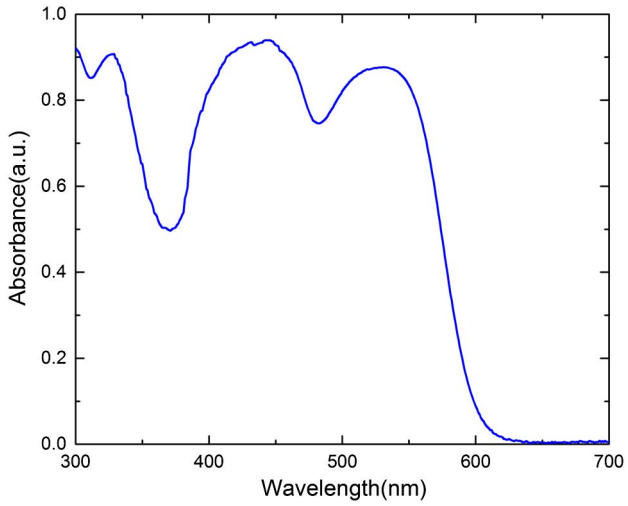

Fig. 2. Absorption spectrum of sample.

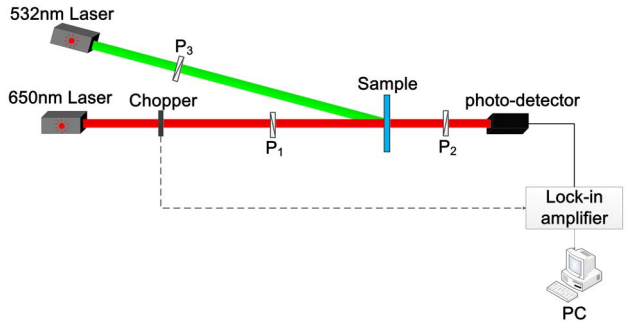

Fig. 3. Setup of the photoinduced birefringence experiment. P1, P2, and P3 refer to polarizer.

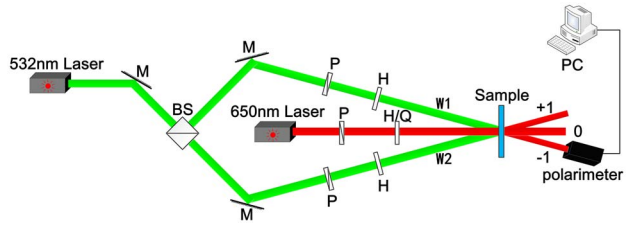

Fig. 4. Experimental setup for polarization grating recording and detection. P, polarizer; BS, beam splitter; M, mirrors; H and Q refer to the half-wave plate and quarter-wave plate, respectively.

orthogonal. The polarization angle of P_3 is set to the middle angle between P_1 and P_2. We measured the transmitted probe light intensity and the initial light intensity. Hence, the photo-induced birefringence can be calculated.

Figure 4 shows the experimental setup for the fabrication and measurement of diffractive wave plates. Two mutually orthogonally circularly polarized (OC mode) 532 nm continuous laser beams are employed as writing beams (W_1 and W_2). Here, W_1 and W_2 refer to right circularly polarized (RC-P) and left circularly polarized (LC-P) beams, respectively. The light intensity of each beam was set to 120 mW/cm^2. The angle between W_1 and W_2 was about 8°. Similarly, we used a continuous 650 nm laser as a real-time probe beam. We measured the transmitted ± first-order probe light intensity and the incident light intensity. The ratio of the two is the diffraction efficiency. By changing the polarization of the incident light and measuring the corresponding polarization of the ± first-order diffraction beam with a polarimeter, we can discover the polarization conversion relationship between the incident beam and the diffraction beam.

All the experiments and metering were carried out at room temperature.

The birefringence induced by the light reflects the light-sensitive properties of the sample. The calculation formula is as

$$I_T = I_0 \sin^2\left(\frac{\pi \Delta n d}{\lambda}\right), \quad (1)$$

where Δn refers to the birefringence value, d refers to the film thickness, λ refers to the wavelength (probe light), I_0 refers to the initial light intensity, and I_T refers to the transmitted probe light intensity. The real-time detected results of photo-induced birefringence are shown in Fig. 5. The "on" and "off" labels represent the switching time of the inducing light. The birefringence value increased with the opening of the inducing light and began to stabilize after reaching the saturation value. With the inducing light closed, the birefringence value reached a stable value after a brief relaxation period. The saturation value of photo-induced birefringence increased with the inducing light intensity. When the inducing light intensity increased to 120 mW/cm^2, a maximum saturation value of $\Delta n = 1.07 \times 10^{-2}$ was achieved. The induced birefringence remains in the sample for several months without attenuation, which is suitable for fabricating diffractive wave plates.

The fabrication of diffracted wave plates is equivalent to the process of polarization holographic recording.

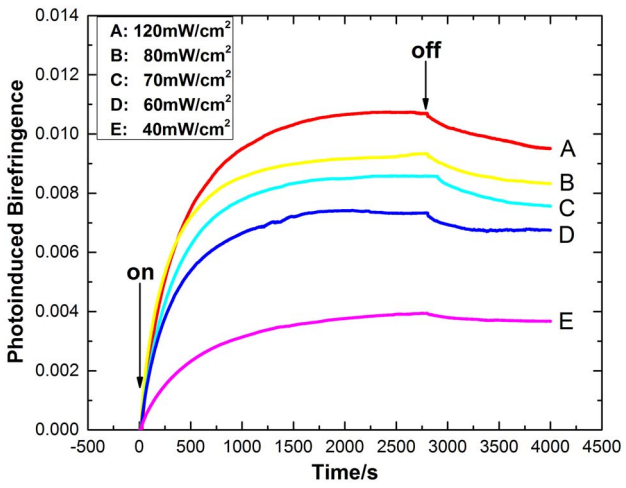

Fig. 5. Temporal behavior of photoinduced birefringence under various pump intensities.

According to Ref. [18], in the case of OC mode recording, the resulting light fields of W_1 and W_2 in space are a sequence of linearly polarized (L-P) regions, as shown in Fig. 6. For the polarization-sensitive materials, a periodic light-induced anisotropy is produced, that is, the polarization holographic grating.

Figure 7 shows the relationship between the diffraction efficiency and recording time using the detecting light of L-P. The "light on" and "light off" labels represent the switching time of the recording light. The diffraction efficiency increased with the opening of the recording light and began to stabilize after reaching the saturation value. With the recording light closed, the diffraction efficiency reached a stable value after a brief relaxation period. The achieved maximum saturation of the + first-order diffraction efficiency is 28.8%. Since the recording light intensity is 120 mW/cm^2, which is consistent with the induced light intensity in a birefringence experiment, we can verify the birefringence value.

For the OC mode recording grating, when the detecting light is L-P light, the diffraction efficiency can be expressed by the following formula[18]:

$$\eta_{\pm 1}(\text{L-P}) = \frac{1}{2}\sin^2\left(\frac{\pi \Delta n d}{\lambda}\right). \tag{2}$$

According to $\eta_{\pm 1}(\text{L-P}) = 0.288$, the value of photo-induced birefringence was calculated to be 1.19×10^{-2}, which was consistent with the result in Fig. 5. It is feasible to fabricate a diffractive wave plate with higher efficiency by inducing a sufficiently large value of photo-induced anisotropy and choosing the appropriate thickness of the sample film.

The recorded grating was found to be highly stable. Thus, the polarization conversion can be conveniently measured. The screenshots of the polarimeter (PAX5710VIS-T, Thorlabs) are shown in Fig. 8. Therefore, the polarization conversion rules of the fabricated diffractive wave plate are summarized. We input L-P light; the + first-order output light was LC-P light, while the other side was RC-P light. We input LC-P light; the + first-order output light was invisible, while the other side was RC-P light. We input RC-P light; the + first-order output light was LC-P light, while the other side was invisible.

The above polarization conversion properties can be explicated using the Jones matrix method[17–19]. The output light fields in the Jones theory are the product of the transmission matrix and the input light. For simplicity, we focus on the polarization information of the output light and just consider the case of linear birefringence. So the first-order output light fields for OC mode recording are

$$E_{\pm 1}(\text{L-P}) = \frac{1}{2}\sin\frac{\Delta\varphi}{2}\begin{pmatrix} \pm\sin\alpha + i\cos\alpha \\ \pm\cos\alpha - i\sin\alpha \end{pmatrix}, \tag{3}$$

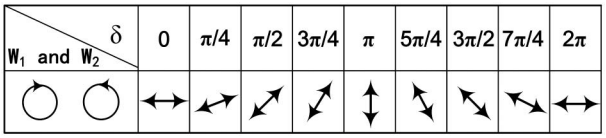

Fig. 6. Polarization modulation of a light field in recording with two waves with orthogonal circularly polarizations (right- and left-hand).

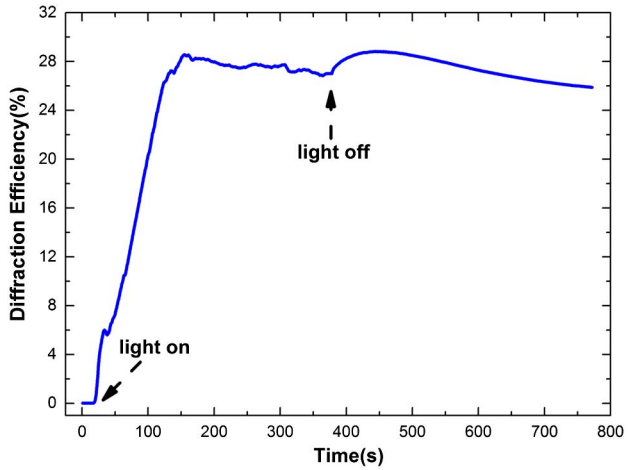

Fig. 7. Real-time behavior of the ± first-order diffraction efficiency in polarization holographic recordings with OC mode.

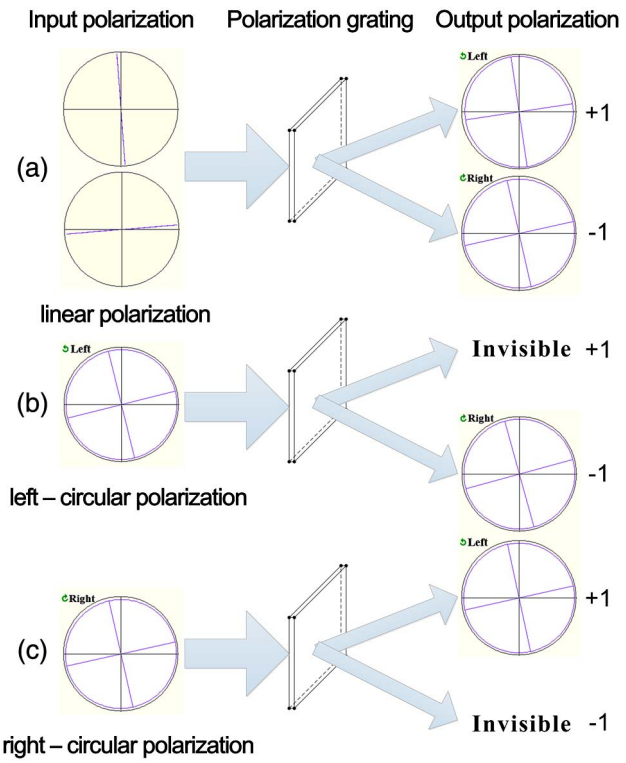

Fig. 8. Polarization conversions for ± first-order diffracted beam. The polarization state images are screenshots obtained from the polarimeter. The upper left corner indicates the polarization direction of the circularly polarized light.

$$E_{+1}(\text{LC-P}) = 0, E_{-1}(\text{LC-P}) = \frac{1}{\sqrt{2}} \sin\frac{\Delta\varphi}{2}\begin{pmatrix} i \\ -1 \end{pmatrix}, \quad (4)$$

$$E_{+1}(\text{RC-P}) = \frac{1}{\sqrt{2}} \sin\frac{\Delta\varphi}{2}\begin{pmatrix} i \\ 1 \end{pmatrix}, E_{-1}(\text{RC-P}) = 0. \quad (5)$$

Thus, we can see that the experiment results were consistent with the analysis.

A highly stable diffractive wave plate is fabricated by two orthogonally circularly polarized 532 nm continuous lasers using polarization holographic techniques. The light-sensitive material we used is an azo polymer with a liquid-crystal structure. The diffractive wave plate can split the incident light into two beams, and alter the polarization state simultaneously, similar to the functional combination of a diffraction grating and a wave plate. The experimental results, which are consistent with the Jones analysis, confirm that the diffractive wave plate converts the incident linear polarization into circular polarization for a L-P probe laser and reverses the sense of rotation of the circular polarization when the detecting light is circularly polarized light. The diffractive wave plate, combined with the advantages of a diffraction grating and a wave plate, can potentially be applied in polarization controlled switching, compact multifunction optical devices, beam shaping, and other fields.

This work was supported by the National Natural Science Foundation of China (Nos. 11174203 and 11574211) and the fund of the State Key Laboratory of Advanced Optical Communication Systems and Networks.

References

1. S. R. Nersisyan, N. V. Tabiryan, D. M. Steeves, and B. R. Kimball, Proc. SPIE **7775**, 777501 (2010).
2. N. V. Tabiryan, S. R. Nersisyan, D. M. Steeves, and B. R. Kimball, Opt. Photonics News **21**, 40 (2010).
3. U. Ruiz, P. Pagliusi, C. Provenzano, V. P. Shibaev, and G. Cipparrone, Adv. Funct. Mater. **22**, 2964 (2012).
4. S. H. D. Kakichashvili, Sov. J. Quantum Electron. **4**, 795 (1974).
5. T. Todorov, L. Nikolova, and N. Tomova, Appl. Opt. **23**, 4309 (1984).
6. M. L. Zheng, X. Xie, Z. Y. Zhang, F. Shi, X. L. Wang, S. C. Fu, and Y. C. Liu, Appl. Opt. **53**, 5815 (2014).
7. X. Xie, M. L. Zheng, S. C. Fu, X. L. Wang, Y. Li, and Y. C. Liu, Opt. Commun. **338**, 269 (2015).
8. S. C. Fu, S. Y. Sun, X. T. Zhang, X. L. Wang, and Y. C. Liu, Opt. Commun. **318**, 1 (2014).
9. S. C. Fu, X. T. Zhang, R. Y. Han, S. Y. Sun, L. L. Wang, and Y. C. Liu, Appl. Opt. **51**, 3357 (2012).
10. X. Zhong, S. Luo, X. Yu, Q. Li, Y. Chen, Y. Sui, and J. Yin, Chin. Opt. Lett. **1**, 414 (2003).
11. G. G. Francisco, D. M. Francisco, and M. Klaus, Nat. Mater. **7**, 490 (2008).
12. T. Sasaki, M. Izawa, K. Noda, E. Nishioka, N. Kawatsuki, and H. Ono, Appl. Phys. B **114**, 373 (2014).
13. F. L. Zhao, C. S. Wang, M. Qin, P. F. Zeng, and P. Cai, Opt. Commun. **338**, 461 (2015).
14. S. H. Lin, S. L. Cho, S. F. Chou, J. H. Lin, C. M. Lin, S. Chi, and K. Y. Hsu, Opt. Express **22**, 14944 (2014).
15. J. Kim, J. H. Suh, B. Y. Lee, S. U. Kim, and S. D. Lee, Opt. Express **23**, 12619 (2015).
16. P. F. Zeng, C. S. Wang, F. L. Zhao, P. Cai, and M. Qin, Appl. Opt. **54**, 53 (2015).
17. H. Ono, A. Emoto, F. Takahashi, N. Kawatsuki, and T. Hasegawa, J. Appl. Phys. **94**, 1298 (2003).
18. X. Pan, C. S. Wang, C. Y. Wang, and X. Q. Zhang, App. Opt. **47**, 93 (2008).
19. X. Liu, B. Y. Wang, and C. S. Guo, Opt. Lett. **39**, 6170 (2014).